Supporting Information

for

A Cholinesterase-Responsive Supramolecular Vesicle

Dong-Sheng Guo, Kui Wang, Yi-Xuan Wang, Yu Liu*

Department of Chemistry, State Key Laboratory of Elemento-Organic Chemistry, Nankai University,

Tianjin, 300071, P. R. China

1. In the absence of SC4A, the optical transmittance of myristoylcholine at 450 nm is not changed versus its increasing concentration from 0.005 to 0.100 mM, indicating that myristoylcholine cannot aggregate in this concentration range.
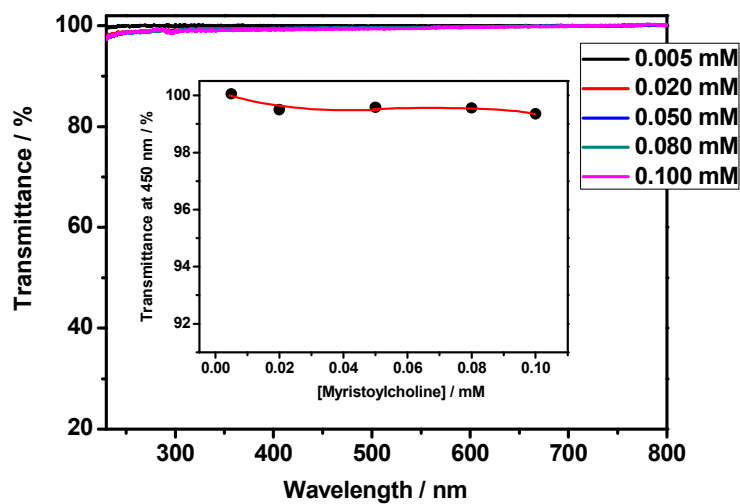

Figure S1. Optical transmittance of aqueous solutions of myristoylcholine at different concentrations at 25 °C. Inset: dependence of the optical transmittance at 450 nm on myristoylcholine concentration.

2. The complexation-induced CAC was obtained according to the plot of optical transmittance at 450 nm versus concentration of myristoylcholine.
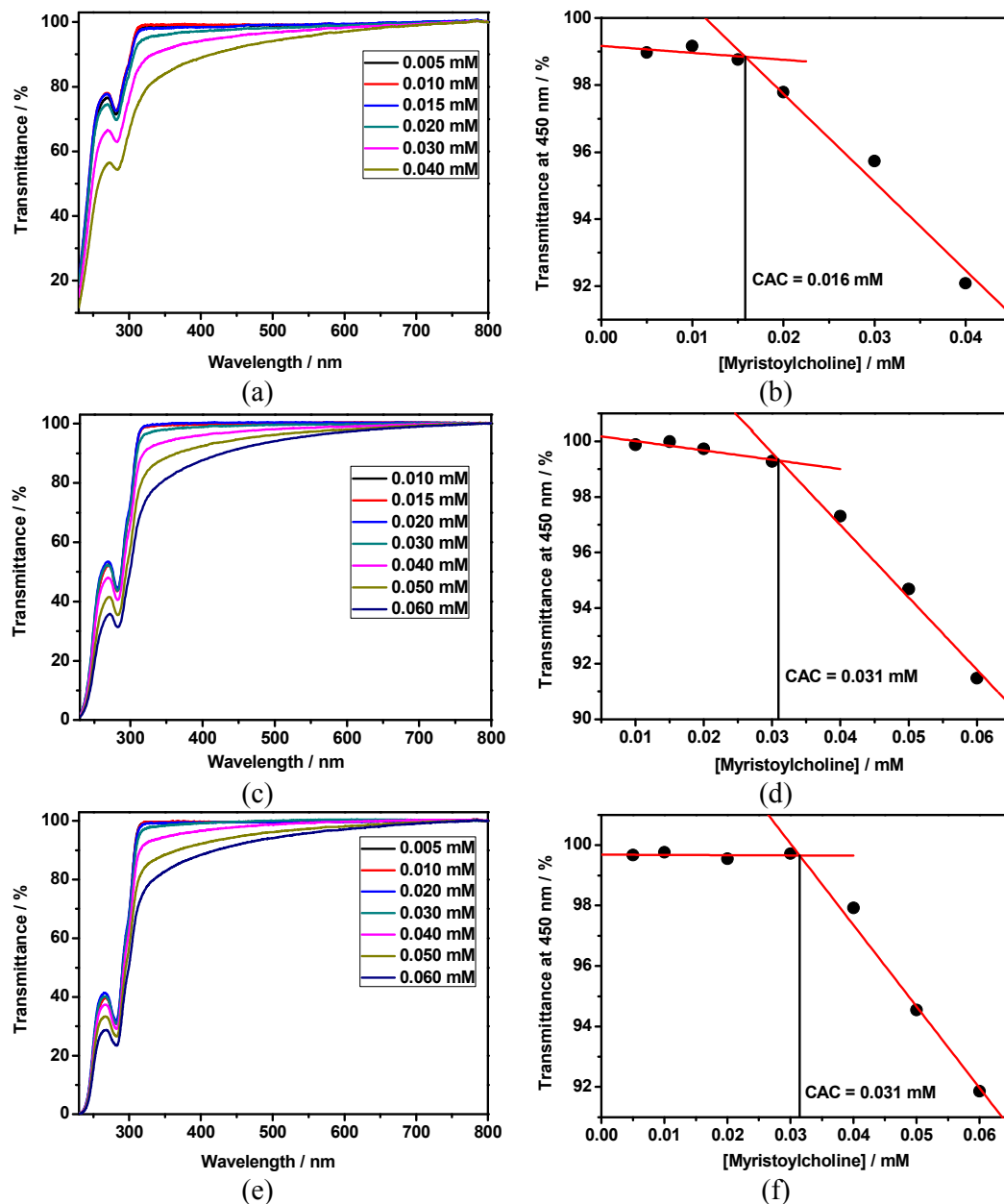

Figure S2. Optical transmittance of aqueous solutions of myristoylcholine at different concentrations in the presence of 0.02 mM (a), 0.05 mM (c), and 0.08 mM (e) SC4A at 25 °C. Dependence of the optical transmittance at 450 nm on myristoylcholine concentration in the presence of 0.02 mM (b), 0.05 mM (d), and 0.08 mM (f) SC4A.

3. Replacement of SC4A by its building subunit 4-phenolsulfonic sodium could not induce the formation of aggregation.
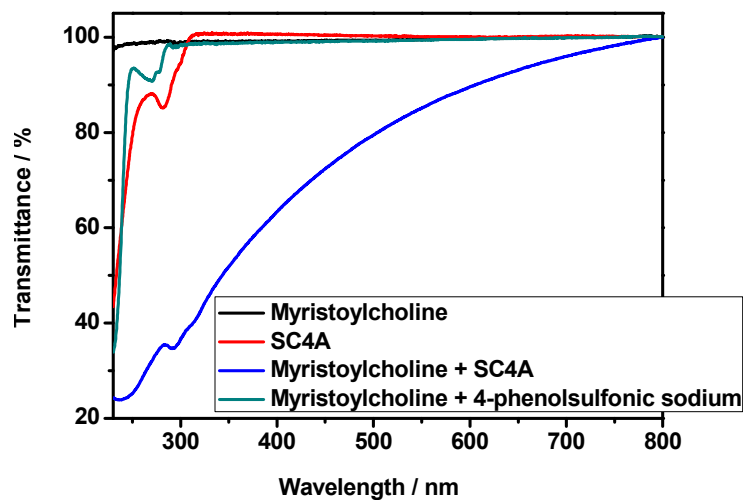

Figure S3. Optical transmittance of myristoylcholine, SC4A, myristoylcholine+SC4A, and myristoylcholine+4-phenolsulfonic sodium at 25 °C in water; [myristoylcholine] = 0.10 mM, [SC4A] = 0.01 mM, [4-phenolsulfonic sodium] = 0.04 mM.

4. TEM image of SC4A+myristoylcholine aggregation at an accelerating voltage of 100 keV.
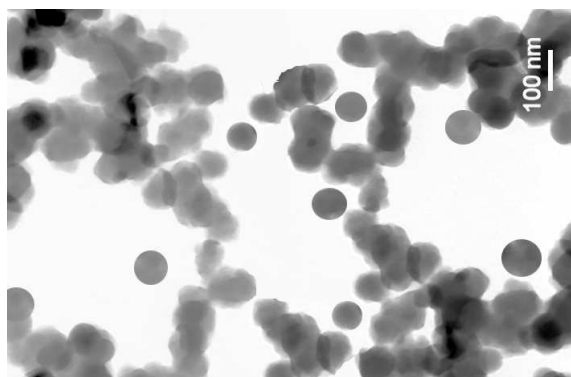

Figure S4. TEM image of SC4A+myristoylcholine aggregationt an accelerating voltage of 100 keV, [myristoylcholine] = 0.10 mM, [SC4A] = 0.01 mM.

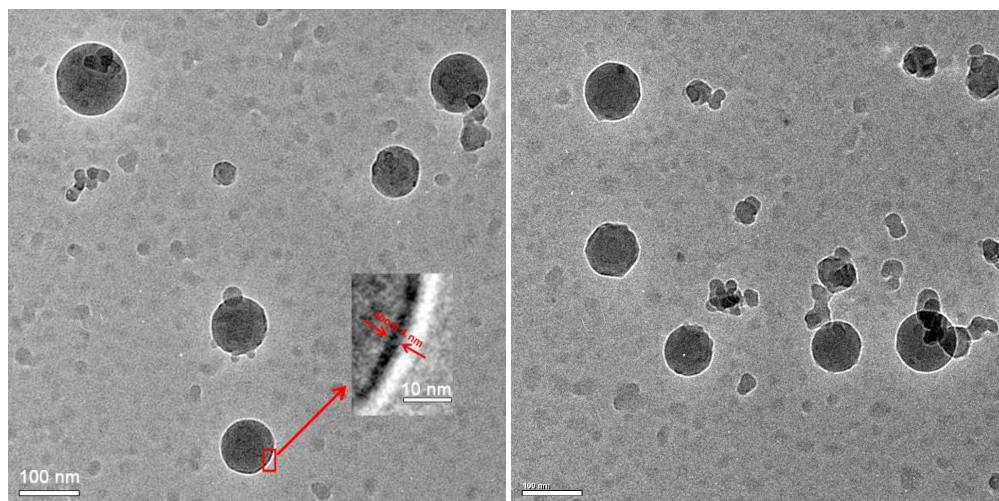**5.** Cryo-TEM image of SC4A+myristoylcholine aggregation.

Figure S5. Cryo-TEM images of SC4A+myristoylcholine assembly. [myristoylcholine] = 0.10 mM, [SC4A] = 0.01 mM.

6. NMR spectroscopy is a powerful tool and has been widely used to determine the structures of calixarene complexes by analyzing the complexation-induced shifts.[1] As shown in the ^{1}H NMR spectra of myristoylcholine in the absence and presence of SC4A in D_2O (Figure S5a), a-H of myristoylcholine exhibited a visible upfield shift ($\Delta\delta$) owing to the ring current effect of the aromatic nuclei of calixarene while the band assigned to the protons of hydrophobic alkyl chain of myristoylcholine (f-H) was not shifted, both of which suggest that the positive quaternary ammonium group of myristoylcholine is encapsulated into the calixarene cavity. It is also noted that, in the absence of SC4A, a simple pattern of sharp signals for the myristoylcholine protons is observed, indicating that myristoylcholine itself exists in the monomeric form at such a high concentration of 1 mM, whereas in the presence of SC4A, the signals are drastically broadened (The bands assigned to b-H, c-H, d-H, e-H, and g-H of myristoylcholine are even not observed.), indicating undoubtedly the stacking of myristoylcholine induced by the complexation of SC4A.

Furthermore, ^{1}H NMR spectra of choline and sodium myristate (the cholinesterase-responsive hydrolysis products of myristoylcholine) in the absence and presence of SC4A were also measured in D_2O (Figure S5b). All choline protons (a-H, b-H, and c-H) exhibited a visible upfield shift ($\Delta\delta$) owing to the ring current effect of the aromatic nuclei of calixarene while all the bands assigned to the protons of sodium myristate (d-H, e-H, f-H, and g-H) were not shifted, which suggests that only choline can be encapsulated into the calixarene cavity after the hydrolysis of myristoylcholine. The $\Delta\delta$ values differ from each other, which can be used to deduce the binding geometry of SC4A-choline complex because the proton with the largest $\Delta\delta$ value would be affected mostly by the ring current effect of the aromatic nuclei of calixarene. The $\Delta\delta$ values of choline protons are in the order of a-H > b-H > c-H, indicating that choline is immersed into the cavity of SC4A in the acclivitous orientation with the positive quaternary ammonium group being included first, which is similar to the binding mode between SC4A and myristoylcholine. However, both the signals for the choline protons and the signals for the sodium myristate protons are not broadened, indicating that sodium myristate cannot aggregate after the

hydrolysis of myristoylcholine, and SC4A and choline can also only form simple 1:1 inclusion complex. It is noted that the $\Delta\delta$ value for the protons of the positive quaternary ammonium group of choline is much larger than that of myristoylcholine, which indicates that myristoylcholine cannot be included into the cavity of SC4A as deep as choline due to the stacking induced by the complexation of SC4A.

NMR: ^{1}H NMR spectra were recorded in D_2O with a Bruker spectrometer (400 MHz) by using DSS as an external reference. The host and guest were mixed in a 1:1 stoichiometry at 1 mM.
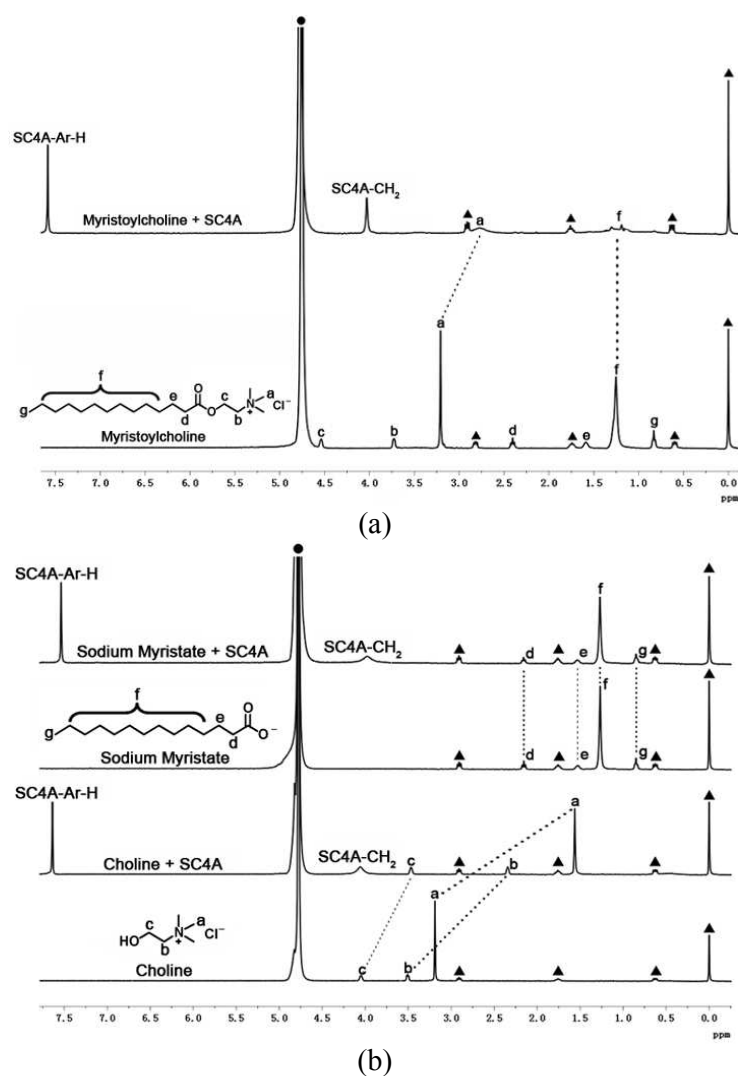

(a)

(b)

Figure S6. (a) ^{1}H NMR spectra of myristoylcholine in the absence and presence of SC4A in D_2O. (b) ^{1}H NMR spectra of choline and sodium myristate in the absence and presence of SC4A in D_2O. DSS (2,2-dimethyl-2-silapentane-5-sulfonate) was added as an external reference. The solvent (H_2O) and DSS are denoted as symbols ● and ▲, respectively.

7. We cannot directly measure the binding constant of SC4A and myristoylcholine because myristoylcholine can aggregate in aqueous solution in the presence of very low amount of SC4A. However, the above NMR results confirm that the binding mode between SC4A and myristoylcholine is similar to that between SC4A and choline (the cholinesterase-responsive hydrolysis product of myristoylcholine). As a result, the binding constant of SC4A and myristoylcholine can be deduced to be in the magnitude of 10^5 M^{-1} according to the binding affinity between SC4A and choline measured by isothermal titration calorimetry, which is also in accordance with the binding constants of SC4A with choline and acetylcholine measured by NMR and fluorescence methods (*ca.* 1.0×10^5 M^{-1}).[2]

Isothermal titration calorimetry: A thermostatted and fully computer-operated isothermal calorimetry (VP-ITC) instrument, purchased from Microcal Inc. (Northampton, MA) was used for all microcalorimetric experiments. The VP-ITC instrument was calibrated chemically by the measurement of the complexation reaction of *β*-cyclodextrin with cyclohexanol, and the obtained thermodynamic data were in good agreement (error < 2%) with the literature data.[3] All microcalorimetric titrations between SC4A and choline were performed in aqueous solution at atmospheric pressure and 298.15 K. Each solution was degassed and thermostatted by a ThermoVac accessory before the titration experiment. Twenty-five successive injections were made for each titration experiment. A constant volume (10 *μ*L / injection) of choline solution in a 0.250 mL syringe was injected into the reaction cell (1.4227 mL) charged with SC4A solution in the same aqueous solution. A representative titration curve was shown in Figure S6. As can be seen from Figure S6, each titration of choline into the sample cell gave an apparent reaction heat caused by the formation of inclusion complex between SC4A and choline. The reaction heat decreases after each injection of choline because less and less SC4A molecules are available to form inclusion complexes. A control experiment was carried out in each run to determine the dilution heat by injecting a choline aqueous solution into a pure aqueous solution containing no SC4A molecules. The

dilution heat determined in these control experiments was subtracted from the apparent reaction heat measured in the titration experiments to give the net reaction heat.

The net reaction heat in each run was analyzed by using the "one set of binding sites" model (ORIGIN software, Microcal Inc.) to simultaneously compute the binding stoichiometry (N), complex stability constant (K_S), standard molar reaction enthalpy ($\Delta H°$), and standard deviation from the titration curve. Generally, the first point of the titration curve was disregarded, as some liquid mixing near the tip of the injection needle is known to occur at the beginning of each ITC run. Knowledge of the complex stability constant (K_S) and molar reaction enthalpy ($\Delta H°$) enabled the calculation of the standard free energy ($\Delta G°$) and entropy changes ($\Delta S°$) according to $\Delta G° = -RT \ln K_S = \Delta H° - T\Delta S°$, where R is the gas constant, and T is the absolute temperature.

A typical curve fitting result for the complexation of choline with SC4A was shown in Figure S7. To check the accuracy of the observed thermodynamic parameters, two independent titration experiments were carried out to afford self-consistent thermodynamic parameters, and their average values with associated errors were listed in Table S1.
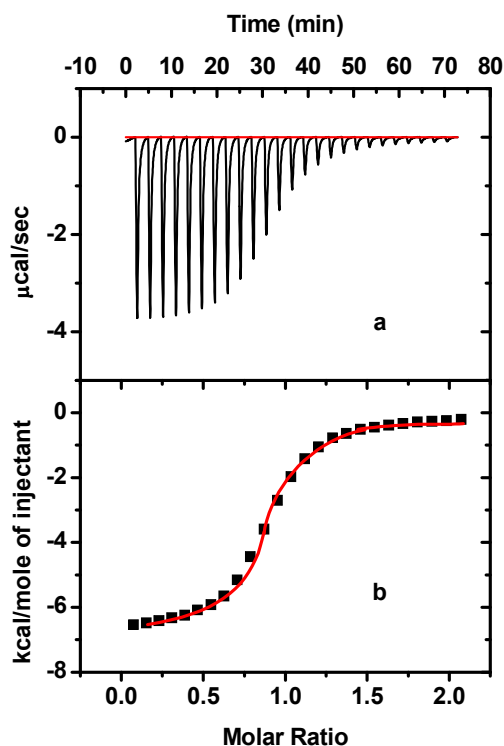
Figure S7. Microcalorimetric titration of SC4A with choline in aqueous solution at 298.15 K. (a) Raw data for 25 sequential injections (10 μL per injection) of a choline solution (2.05 mM) into a SC4A solution (0.17 mM). (b) Apparent reaction heat obtained from the integration of the calorimetric traces.
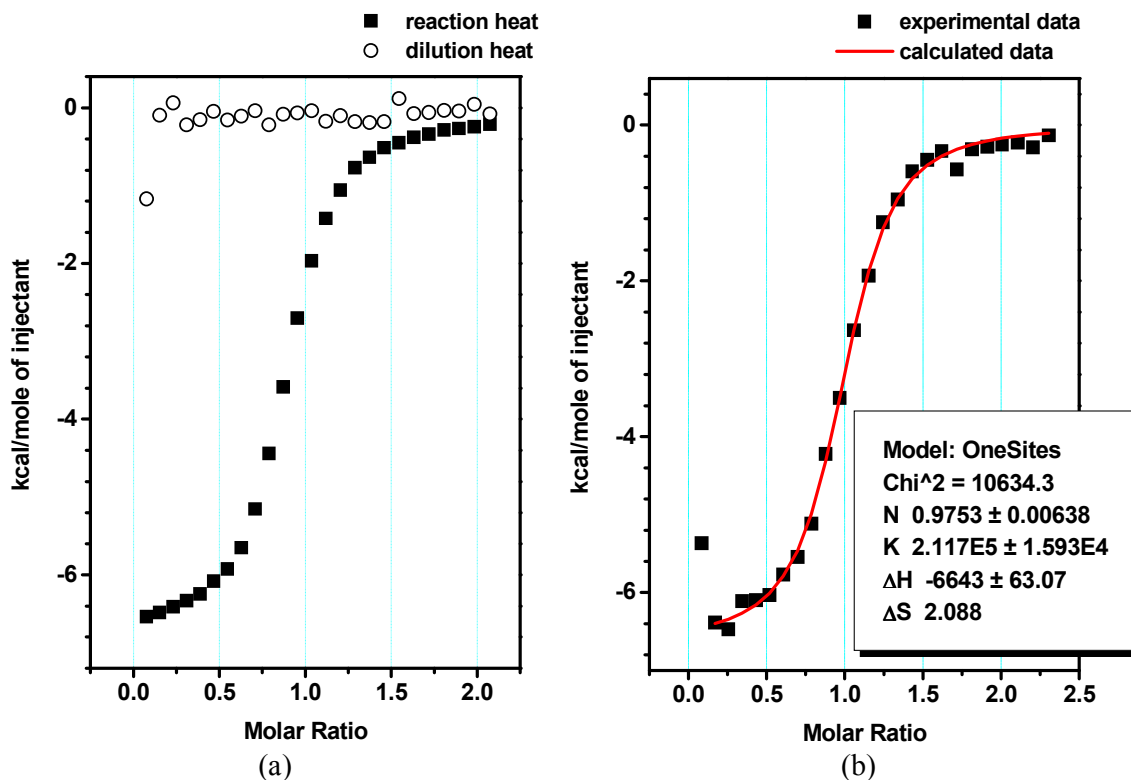

(a)   (b)

Figure S8. (a) Heat effects of the dilution and of the complexation reaction of choline with SC4A for each injection during isothermal titration microcalorimetric experiment. (b) "Net" heat effects of complexation of choline with SC4A for each injection, obtained by subtracting the dilution heat from the reaction heat, which was fitted by computer simulation using the "one set of binding sites" model.

Table S1. Complex Stability Constants (K_S/M^{-1}), Enthalpy ($\Delta H°/(kJ\cdot mol^{-1})$), and Entropy Changes ($T\Delta S°/(kJ\cdot mol^{-1})$) for 1:1 Intermolecular Complexation of Choline with SC4A in Aqueous Solution at 298.15 K.

Complexes	K_S	$\Delta H°$	$T\Delta S°$
SC4A + Choline	$(2.17\pm0.05) \times 10^5$	-27.56 ± 0.20	2.86 ± 0.26

8. The optical transmittance of SC4A+myristoylcholine aggregation was not changed significantly within 24 hours, indicating that the resulting vesicles are stable and the vesicular structure can be maintained at least over 24 hours.
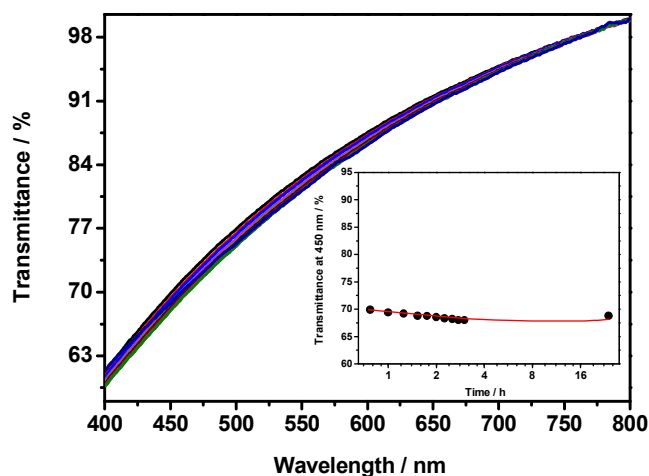

Figure S9. Optical transmittance of SC4A+myristoylcholine aggregation at different time within 24 hours at 25 °C. Inset: dependence of the optical transmittance at 450 nm on time, [myristoylcholine] = 0.10 mM, [SC4A] = 0.01 mM.

9. The optical transmittance of SC4A+myristoylcholine aggregation increases systematically with time in the presence of 0.5 U/mL BChE.
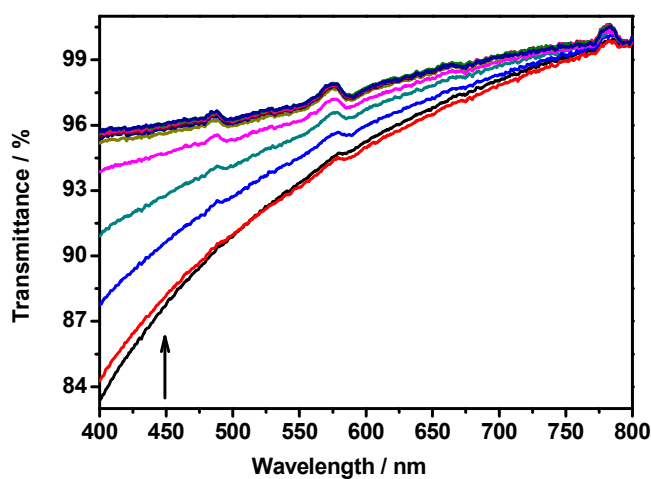

Figure S10. Optical transmittance of SC4A+myristoylcholine aggregation at different time within 3 hours in the presence of 0.5 U/mL BChE, [myristoylcholine] = 0.10 mM, [SC4A] = 0.01 mM.

10. The formation and disassembly of SC4A+myristoylcholine vesicles can also be achieved in normal saline.
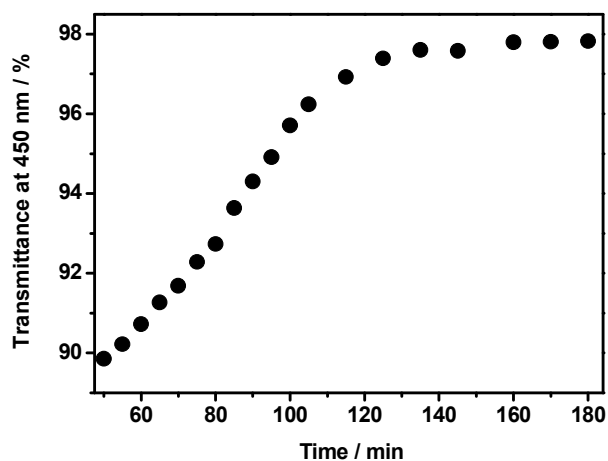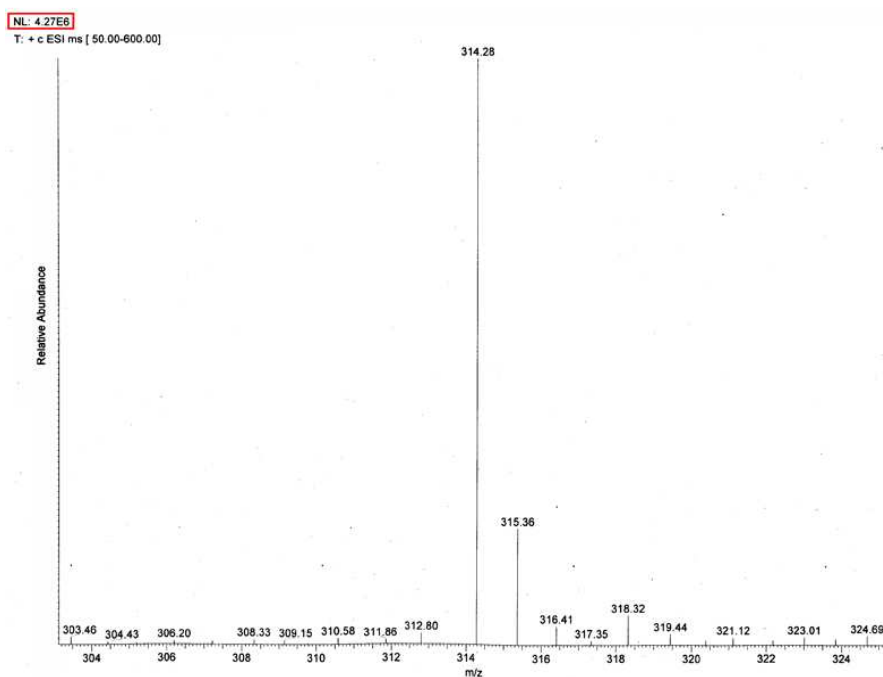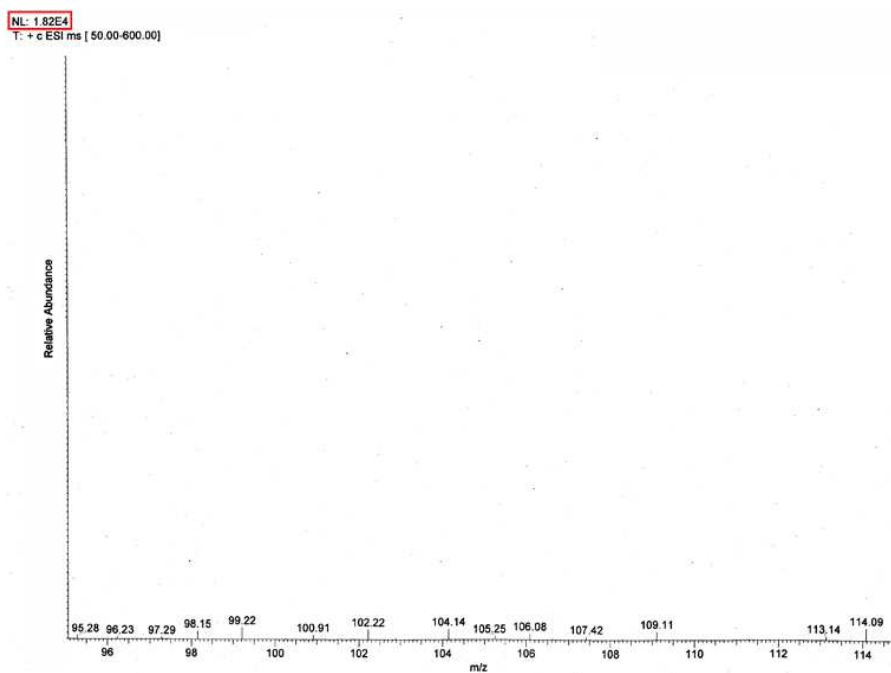

Figure S11. Dependence of the optical transmittance of SC4A+myristoylcholine aggregation at 450 nm on time in the presence of BChE in normal saline, [myristoylcholine] = 0.10 mM, [SC4A] = 0.01 mM, [BChE] = 0.5 U/mL.

11. Mass spectrum measurements were performed to demonstrate enzymatic cleavage of the ester bonds of myristoylcholine molecules in the supramolecular vesicles. Figures S11a-c show mass spectra of myristoylcholine (a) and its cholinesterase-responsive hydrolysis products (choline (b) and sodium myristate (c)), in which the signal for the peak assigned to [myristoylcholine]$^+$ (peak at 314 (a)) is strong while the signals for the peaks assigned to[choline]$^+$ (peak at 104 (b)) and [myristate]$^-$(peak at 227 (c)) are so weak. As a result, the peak at 314 which is assigned to [myristoylcholine]$^+$ was used to detect enzymatic cleavage of the ester bonds of myristoylcholine molecules in the supramolecular vesicles. Figures S11d-g show the mass spectra of SC4A+myristoylcholine aggregation at different time after addition of BChE. After 5 hours the peak at 314 was obviously weakened, and 12.5 hours later this peak almost disappeared, thus indicating that all of the ester bonds had been cleaved.
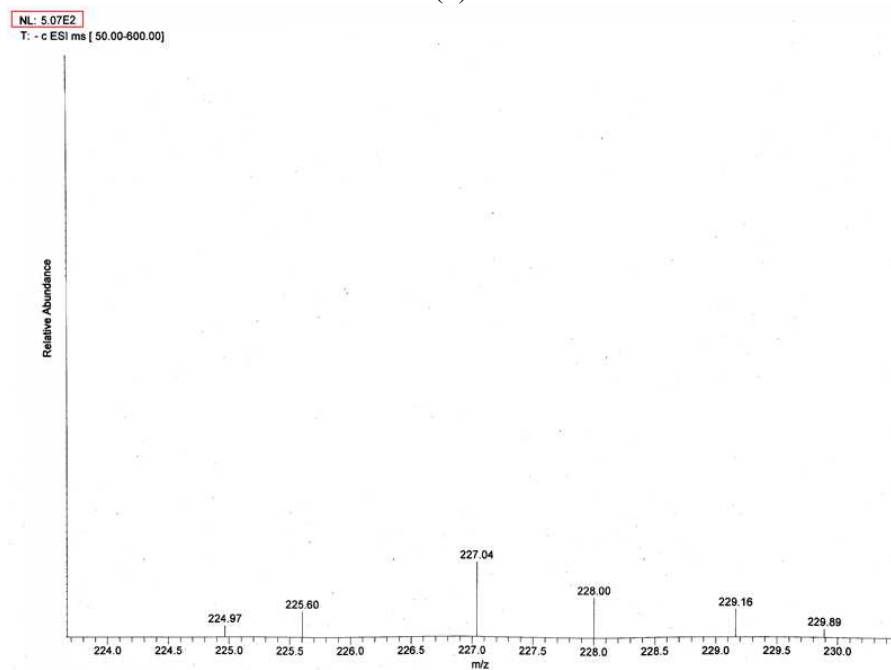
Mass spectra: Mass spectra were recorded with an IonSpec QFT-ESI MS with the same amount of sample.
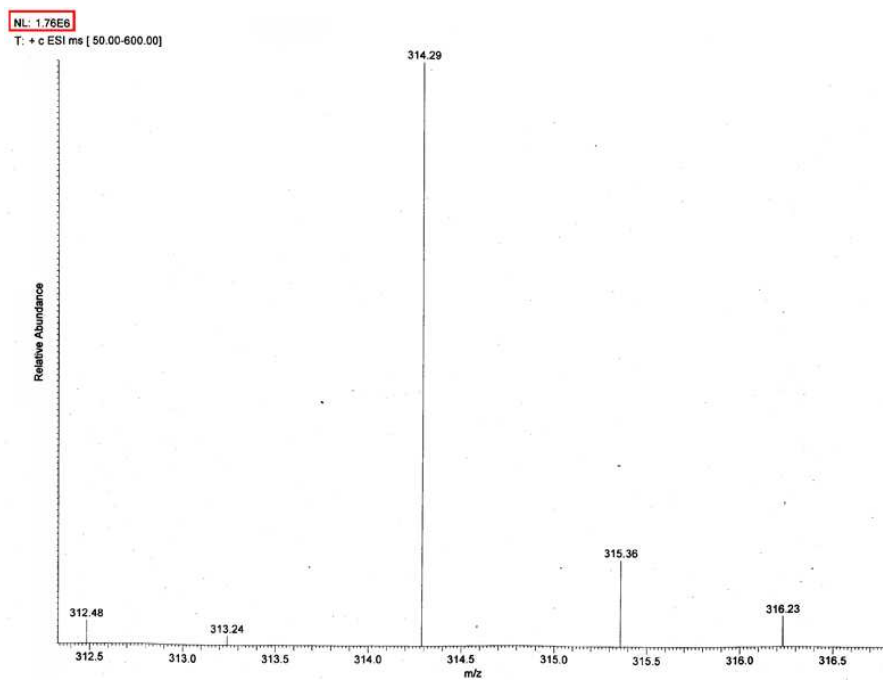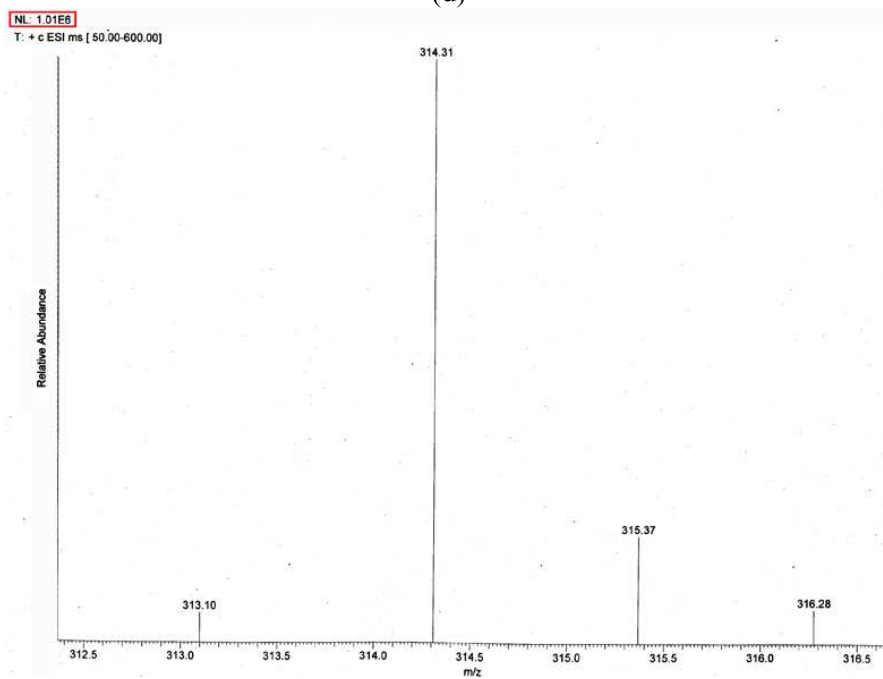

(a)

Relative Abundance

95.28 96.23 97.29 98.15 99.22   100.91 102.22 104.14 105.25 106.08 107.42   109.11   113.14 114.09

96   98   100   102   104   106   108   110   112   114

m/z

(b)

Relative Abundance

224.97   225.60   227.04   228.00   229.16   229.89

224.0 224.5 225.0 225.5 226.0 226.5 227.0 227.5 228.0 228.5 229.0 229.5 230.0
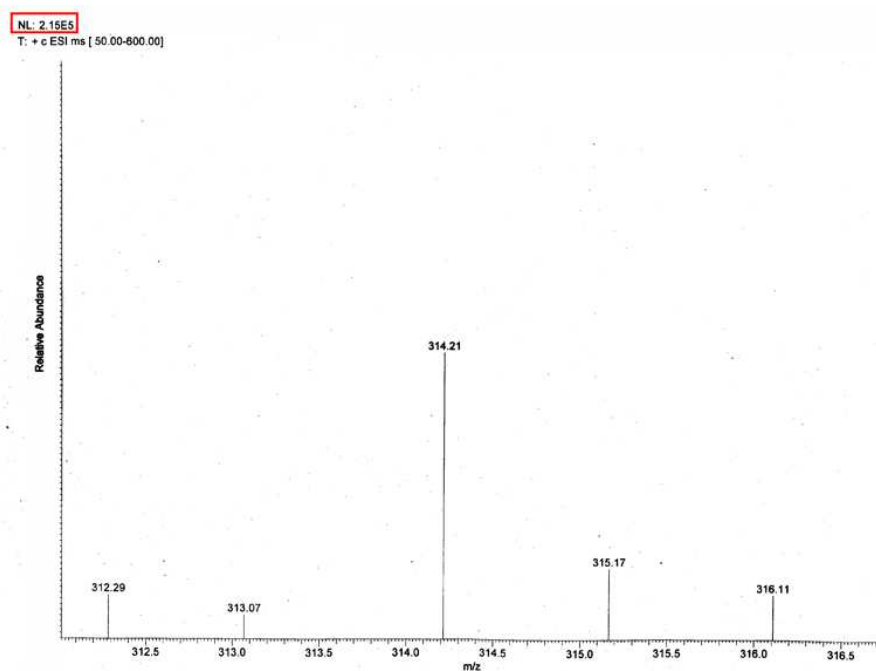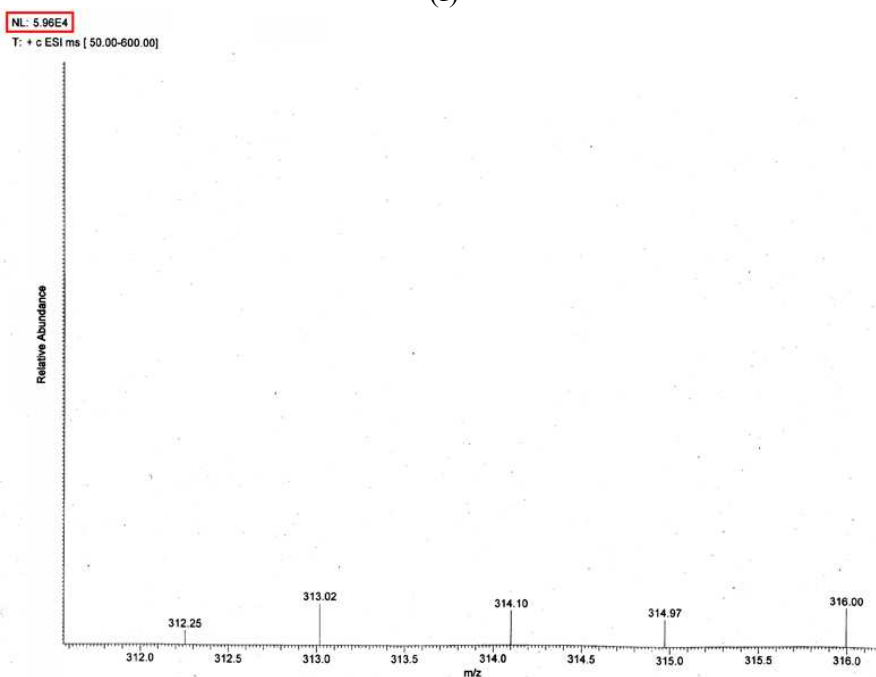
m/z

(c)

(d)

(e)

(f)

(g)

Figure S12. ESI-MS of a solution containing myristoylcholine (a), choline (b), and sodium myristate (c) in water. The peaks at 314 (a), 104 (b), and 227 (c) were assigned to [myristoylcholine]$^+$, [choline]$^+$, and [myristate]$^-$, respectively. ESI-MS of a solution containing SC4A+myristoylcholine aggregation at different time after addition of BChE (0.5 h for (d), 3 h for (e), 5 h for (f), and 12.5 h for (g)).

12. The optical transmittance of SC4A+myristoylcholine aggregation increases faster with time in the presence of more amount of enzyme, indicating that the rate for the cholinesterase-responsive disassembly of the vesicles is related to the concentration of added enzyme and more amount of enzyme would trigger a faster disassembly.
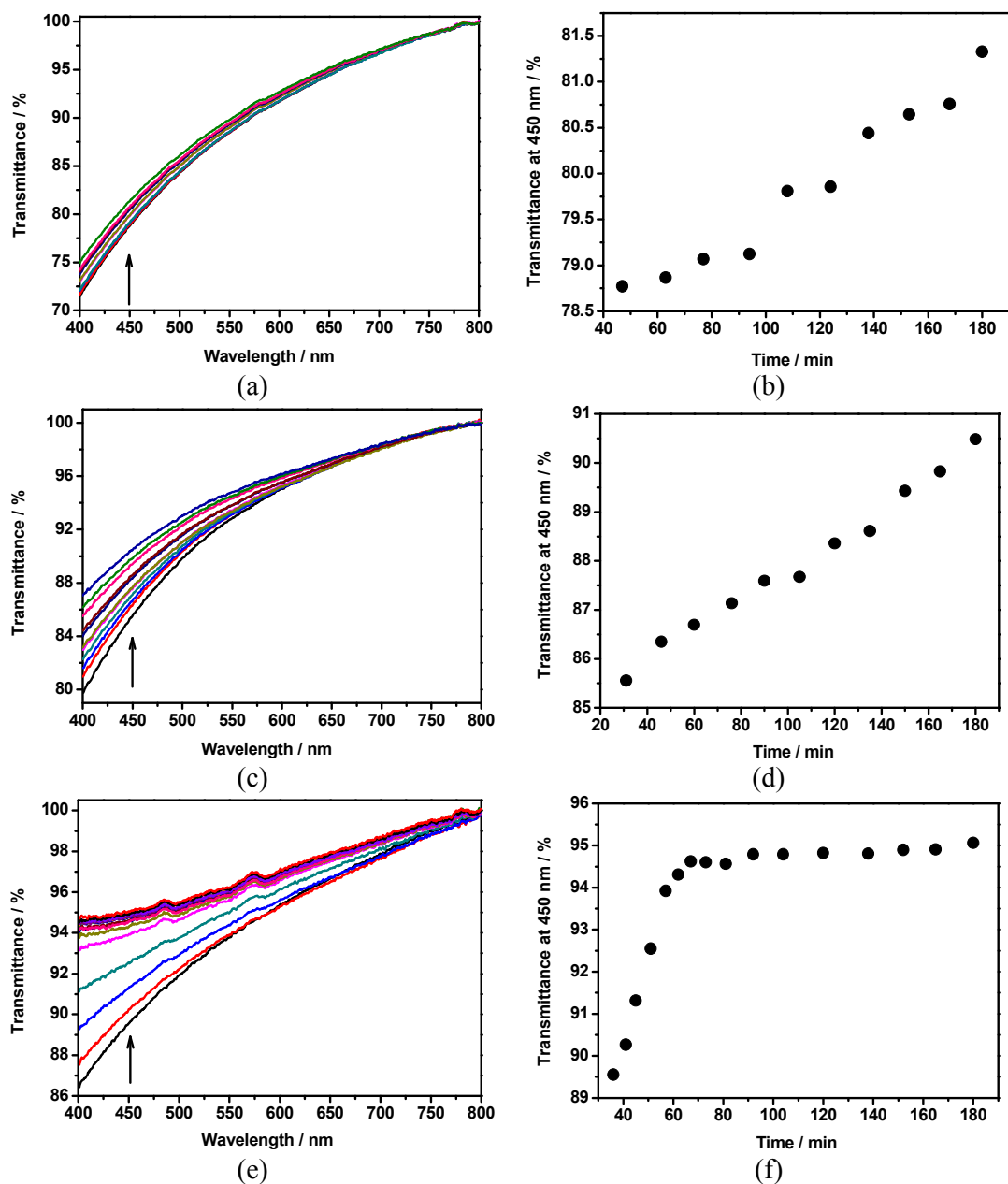

Figure S13. Optical transmittance of SC4A+myristoylcholine aggregation at different time within 3 hours in the presence of 0.1 U/mL (a), 0.3 U/mL (c), and 0.8 U/mL (e) BChE. Dependence of the optical

transmittance of SC4A+myristoylcholine aggregation at 450 nm on time in the presence of 0.1 U/mL (b), 0.3 U/mL (d), and 0.8 U/mL (f) BChE. [myristoylcholine] = 0.10 mM, [SC4A] = 0.01 mM.

13. There was no significant change with time in optical transmittance for SC4A+myristoylcholine vesicle in the presence of denatured BChE, thus eliminating the possibility of the enzyme protein BChE itself being a factor that contributes to the change in SC4A+myristoylcholine system.
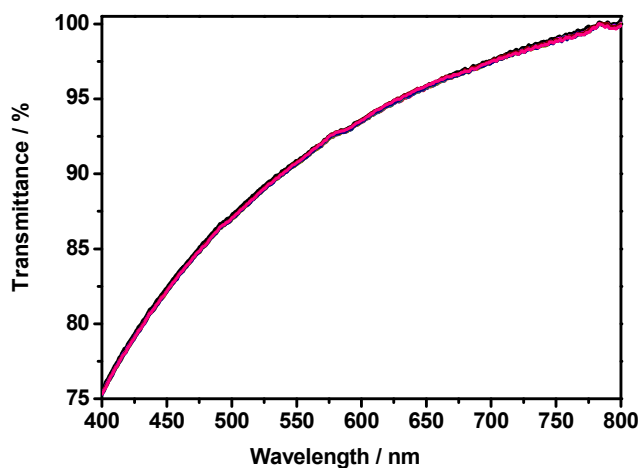

Figure S14. Optical transmittance of SC4A+myristoylcholine aggregation at different time within 3 hours in the presence of 0.5 U/mL denatured BChE, [myristoylcholine] = 0.10 mM, [SC4A] = 0.01 mM.

14. In the presence of CIAP/Exo I/GOx, there was no significant change with time in either the optical transmittance or the Tyndall effect, demonstrating that this enzyme-responsive vesicle exhibits good selectivity toward cholinesterase.
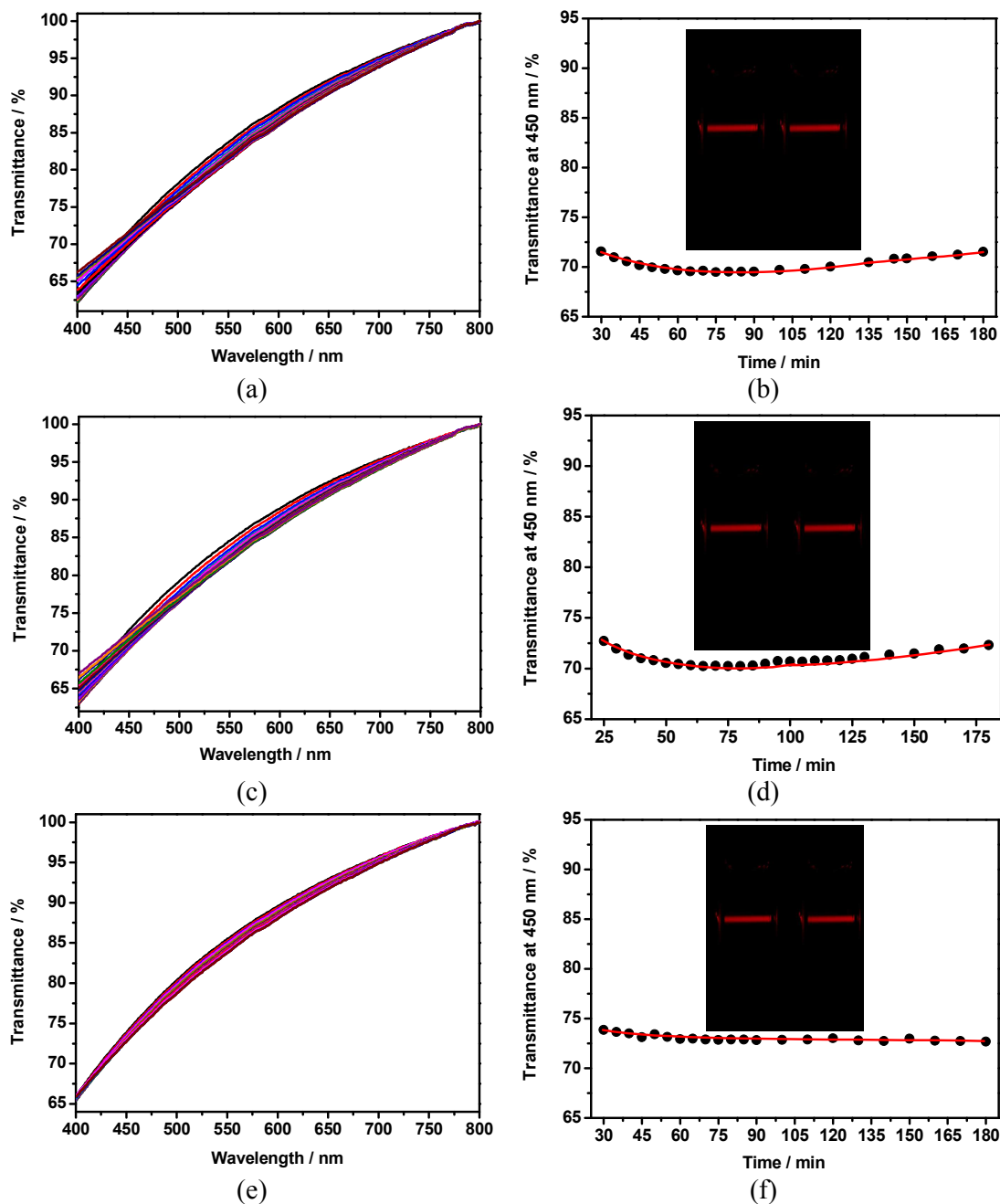

Figure S15. Optical transmittance of SC4A+myristoylcholine aggregation at different time within 3 hours in the presence of 0.5 U/mL CIAP (a), Exo I (c), and GOx (e). Dependence of the optical transmittance of SC4A+myristoylcholine aggregation at 450 nm on time in the presence of 0.5 U/mL CIAP (b), Exo I (d), and GOx (f). Inset: Tyndall effect of SC4A+myristoylcholine aggregation before

(left) and after (right) addition of 0.5 U/mL CIAP (b), Exo I (d), and GOx (f) for 3 hours. [myristoylcholine] = 0.10 mM, [SC4A] = 0.01 mM.

15. Controllable HPTS release: An excitation wavelength of 339 nm and an emission wavelength of 512 nm were used. The initial fluorescence intensity (F_0) of HPTS-loaded vesicles was measured by using a fluorescence spectrometer, and then the fluorescence intensity (F_t) of HPTS-loaded vesicles in the absence and presence of BChE was measured as a function of time. In another independent experiment, the fluorescence intensity ($F_{t'}$) of HPTS-loaded vesicles was measured 4 hours later after addition of different concentrations of BChE or GOx. Finally, the overall fluorescence intensity (F_{max}) was measured and the release percentage of HPTS-loaded vesicles was calculated by using Equation (1):

$$\text{Release percentage (\%)} = (F_{t(t')} - F_0) / (F_{max} - F_0) \times 100 \quad (1)$$

The reason for the quenching of fluorescence emission of HPTS in the vesicles may be the self-quenching originating from its relatively high concentration in the vesicles or the photoinduced electron transfer from the oxygen anion at the lower-rim of SC4A to HPTS. The pH value for this SC4A+myristoylcholine system is 6.8. According to the pK_a values of lower-rim phenolic hydroxyl groups of SC4A (pK_a values = 3.08, 12.02),[4] at least one phenol group is deprotonated at this pH value.
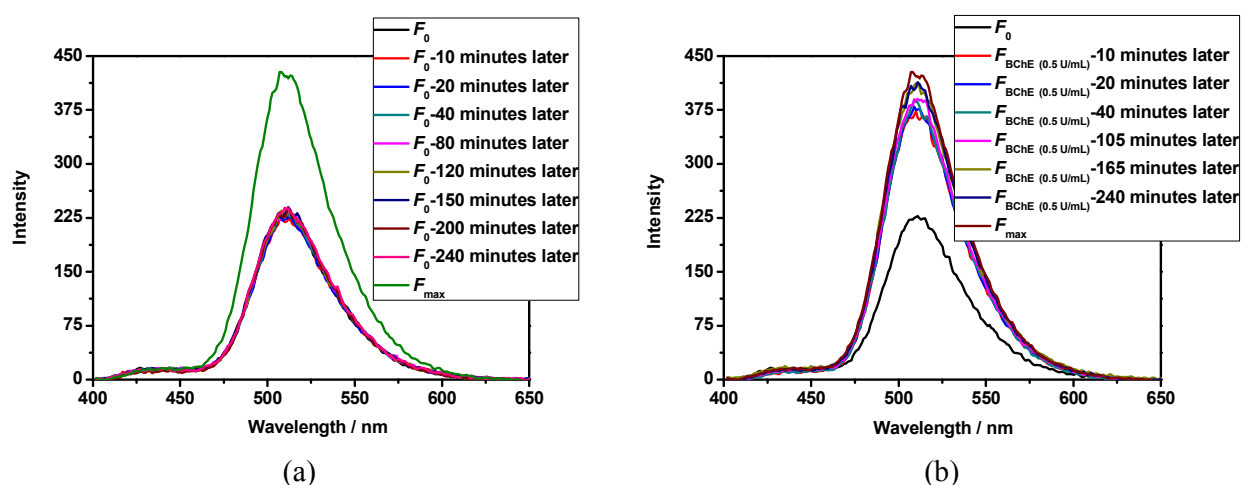

(a)　　　　　　　　　　(b)

Figure S16. Fluorescence emission spectra of HPTS-loaded vesicle at different time within 4 hours in the absence (a) and in the presence (b) of BChE, [BChE] = 0.5 U/mL.
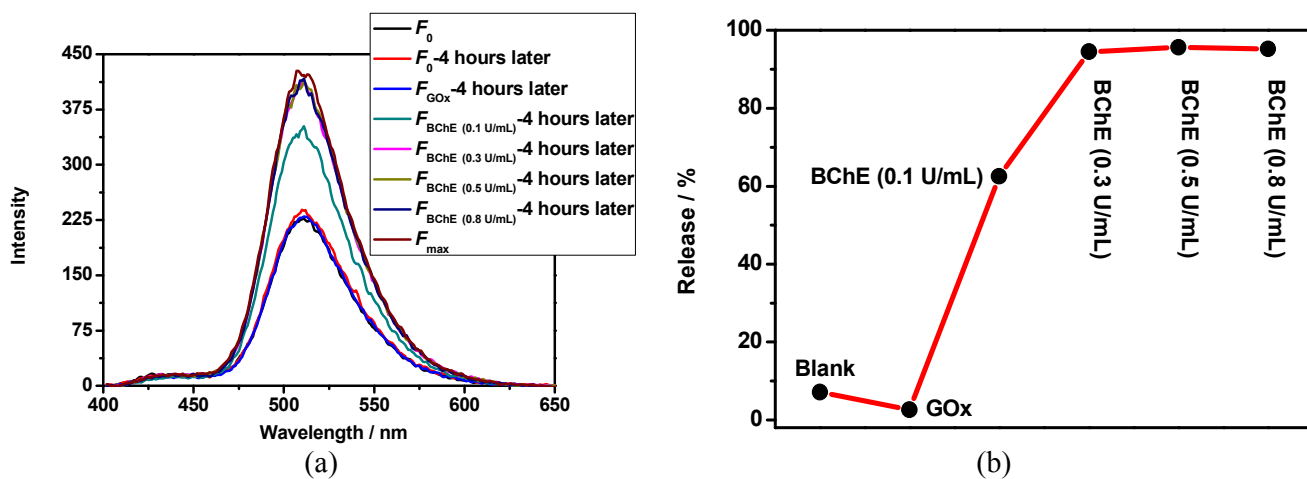
Figure S17. (a) Fluorescence emission spectra of HPTS-loaded vesicle 4 hours later after addition of different concentrations of BChE or GOx, [GOx] = 0.5 U/mL. (b) Release of HPTS encapsulated in the supramolecular vesicle formed by SC4A+myristoylcholine 4 hours later after addition of different concentrations of BChE or GOx.

16. The tacrine-loaded vesicle can also disassemble in the presence of 0.5 U/mL BChE while the disassembly cannot occur in the presence of denatured BChE. Differently, tacrine-loaded vesicles cannot disassemble fully like unloaded vesicles.
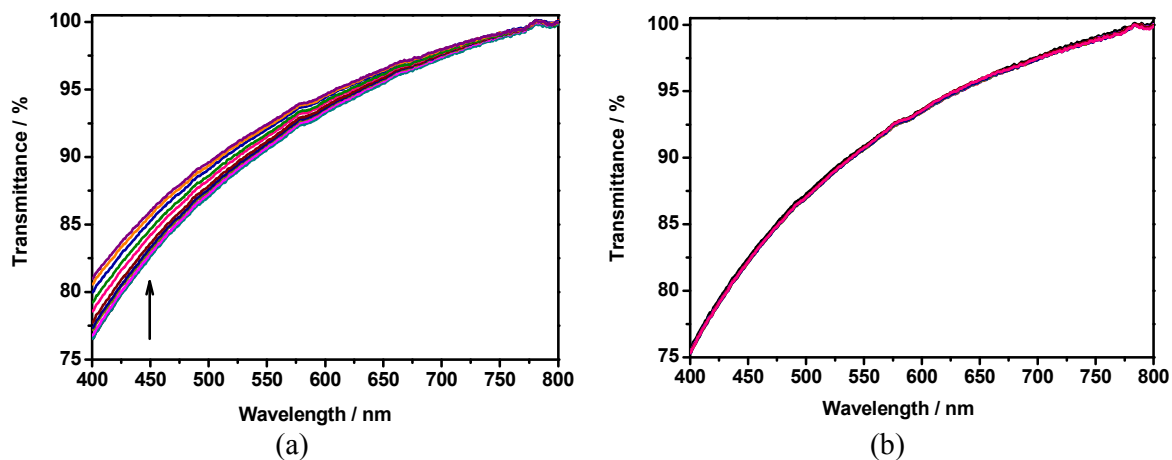

(a)   (b)

Figure S18. Optical transmittance of tacrine-loaded vesicle at different time within 3 hours in the presence of 0.5 U/mL BChE (a) and denatured BChE (b).

17. The images of living LO2 cells in blank and SC4A+myristoylcholine vesicle group.
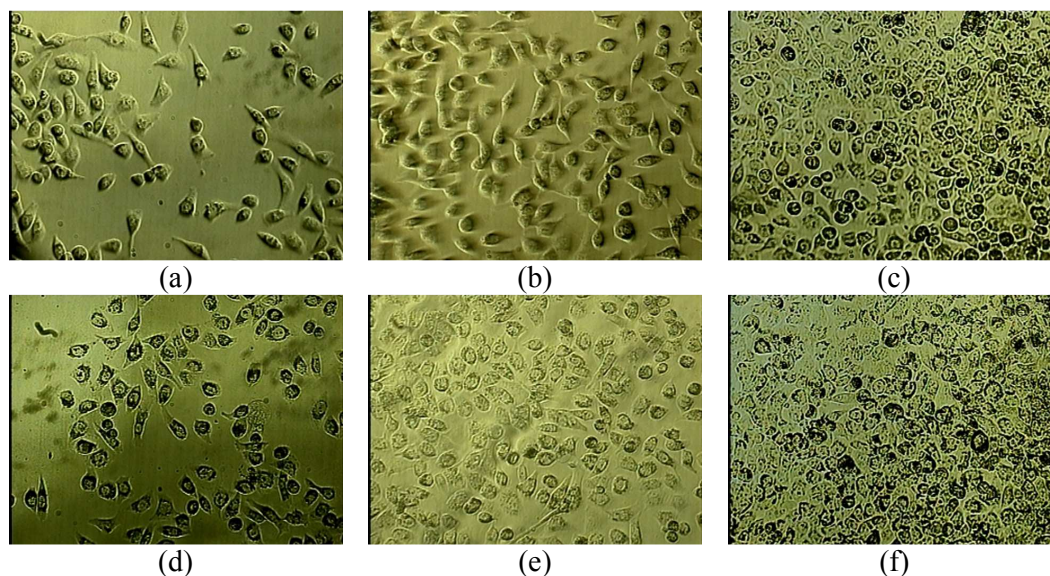

Figure S19. The images of living LO2 cells in blank (a-c) and SC4A+myristoylcholine vesicle (d-f) group after 24 (a and d), 48 (b and e), and 96 (c and f) hours.

References

[1] S. Shinkai, K. Araki, T. Matsuda, N. Nishiyama, H. Ikeda, I. Takasu, M. Iwamoto, *J. Am. Chem. Soc.* **1990**, *112*, 9053–9058.

[2] a) D.-S. Guo, V. D. Uzunova, X. Su, Y. Liu, W. M. Nau, *Chem. Sci.* **2011**, *2*, 1722–1734; b) H. Bakirci, W. Nau, M. *Adv. Funct. Mater.* **2006**, *16*, 237–242; c) J.-M. Lehn, R. Meric, J.-P. Vigneron, M. Cesario, J. Guilhem, C. Pascard, Z. Asfari, J. Vicens, *Supramol. Chem.* **1995**, *5*, 97–103.

[3] M. V. Rekharsky, Y. Inoue, *Chem. Rev.* **1998**, *98*, 1875–1917.

[4] H. Matsumiya, Y. Terazono, N. Iki, S. Miyano, *J. Chem. Soc., Perkin Trans. 2* **2002**, 1166–1172.